Journal of Sustainable Development of Energy, Water and Environment Systems

http://www.sdewes.org/jsdewes

Year 2026, Volume 14, Issue 3, 1140714

Original Research Article

Iterative Optimization Approach for Sizing Standalone Photovoltaic Systems with Energy Storage Battery Integrating a Predictive Battery Aging Model

Guétinsom Jean Kafando, Daniel Yamegueu*

Département Génie Electrique Energétique et Industriel, Laboratoire Energies Renouvelables et Efficacité Energétique, Institut International d'Ingénierie de l'Eau et de l'Environnement(2iE), Rue de la Sciences, Ouagadougou, Burkina Faso

e-mail: jean.kafando@2ie-edu.org, daniel.yamegueu@2ie-edu.org

Cite as: Kafando, G. J., Yamegueu, D., Iterative Optimization Approach for Sizing Standalone Photovoltaic Systems with Energy Storage Battery Integrating a Predictive Battery Aging Model, J.sustain. dev. energy water environ. syst., 14(3), 1140714, 2026, https://doi.org/10.13044/j.sdewes.d14.0714

ABSTRACT

This work optimizes the conventional intuitive sizing method for standalone photovoltaic systems with energy storage, still widely used despite its limitations, particularly neglecting battery aging. It often leads to oversized storage and higher costs due to excessive autonomy days assumptions. This paper proposes an improved iterative approach based on hourly irradiance and consumption profiles while integrating a predictive battery aging model to enhance system reliability and economic feasibility. A global energy model, performance indicators, a battery aging model, and a MATLAB algorithm were developed. A simulation for a 4.5 kWh/day consumption in a peri-urban area of Ouagadougou, Burkina Faso, yielded an optimal configuration: a 1060 W_p Photovoltaic generator and a 100.60 Ah storage renewed every two years, covering 90% of demand at 0.20 EUR/kWh. This approach reduces the storage size by 35.92% and the Levelized Cost of Energy by 37.50% compared to the conventional method.

KEYWORDS

Standalone system, PV system, Storage battery, Sizing, Optimization, Aging.

INTRODUCTION

The 7th Sustainable Development Goal (SDG 7), adopted in 2015 by the United Nations, aims to ensure universal access to reliable, sustainable, and affordable energy services by 2030 [1]. In [2] it's even mentioned that success in most of the remaining 16 Sustainable Development Goals depends on access to energy too. To achieve this goal, the use of standalone microgrids or autonomous photovoltaic (PV) systems with battery energy storage is strongly encouraged by the International Energy Agency in areas with high solar potential and no access to the public electricity grid [3]. Standalone PV system with storage is considered as a promising application in locations where grid extension is uneconomical, specially, in rural areas as it is mentioned in [4].

In Sub-Saharan Africa where approximately 80% of the population living in rural areas still lacks electricity [5]. However, the large-scale adoption of standalone PV systems with storage remains limited despite abundant solar energy availability [6].This is mainly due to technical

* Corresponding author

reliability and economic accessibility challenge, attributed to the high cost of components especially storage batteries and improper system sizing [7]. Undersizing increases power shortages for users, while oversizing leads to unnecessary economic costs. Consequently, the challenge of ensuring both technical reliability and economic affordability of standalone PV systems has made system sizing a critical research issue, leading to the development of various sizing methodologies in the literature.

A review of several sizing approaches for standalone PV systems have therefore been proposed in [8] and [9]. These approaches have been classified in [7] into three main families: (i) conventional intuitive or static methods, (ii) conventional dynamic methods, including numerical, analytical, and probabilistic approaches, and (iii) artificial intelligence–based methods, such as genetic algorithms and particle swarm optimization.

The conventional intuitive or static method relies on averaged values (solar irradiation and user energy needs) and doesn't account for resources and demand temporal variability [10]. Moreover, unrealistic storage autonomy assumptions are used and often lead to excessive storage and higher costs as it's mentioned in [10]. For example, studies [11] and [12] recommend autonomy ranges of 2 to 9 days and 3 to 5 days. In [8] the intuitive method is presented as a simple and practical solution for preliminary sizing, particularly when load and solar irradiation data are limited.

However, due to the limitations of this static approach especially its inability to represent temporal variability and the real operating behavior of system components dynamic sizing methods have progressively been developed to improve the technical reliability and economic viability of standalone PV systems [13]. Generally built upon the conventional intuitive method for initial pre-sizing, these dynamic approaches exploit hourly time-series data of solar irradiance, temperature, and electricity consumption. They enable the coupling of technical system variables (PV generator and storage sizes) with economic variables (component costs) within a techno-economic sizing framework, using performance indicators such as the Loss of Power Supply Probability (*LPSP*) and the Levelized Cost of Energy (*LCOE*).

Nevertheless, these dynamic methods have been criticized for their limited flexibility and, in some cases, reduced accuracy, which has led to the emergence of artificial intelligence (AI)-based approaches, also referred to as next-generation methods [14]. Artificial intelligence techniques such as genetic algorithms, particle swarm optimization, and neural networks are now widely applied to the optimal sizing of power generation systems, particularly standalone PV systems with battery storage. Their main advantage lies in their high flexibility and ability to explore large solution spaces [15].

However, these methods do not always lead to truly optimal solutions or even fail to converge, mainly due to the probabilistic nature of their implementation, such as the arbitrary selection of crossover and mutation probabilities in genetic algorithms, which remain among the most widely used AI techniques [16]. These limitations have motivated several authors to propose hybrid approaches that not only combine different artificial intelligence techniques but also integrate AI-based methods with conventional numerical and deterministic approaches, in order to enhance the robustness, accuracy, and reliability of the obtained results. This is the case in studies conducted in [17] and [18].

Moreover, due to a certain degree of skepticism toward artificial intelligence methods, many recent studies continue to develop new dynamic sizing approaches based on the classical intuitive method, aiming to achieve optimal sizing of standalone PV systems with battery storage. Such a sizing technic has been proposed in [19] and [20]. However, most of these approaches do not account for realistic battery aging analysis in the prediction of storage lifetime, even though this parameter plays a key role in the evaluation of the Levelized Cost of Energy (*LCOE*).

In [21] it's revealed the existence of several battery lifetime prediction models such as the rainflow algorithm recognized to be simple and accurate. However, their explicit integration in renewable energy systems sizing methods is not yet effective. This omission or the direct use of

storage lifetime values provided by manufacturers under specific conditions (regular cycling), may result in either underestimation or overestimation of the system *LCOE*, owing to the irregular cycling of storage caused by solar resource fluctuations [22].

In addition, some studies have considered the autonomy duration as an optimization variable, but without accounting for the actual aging of the storage system [23], while others have been limited to a sensitivity analysis of the autonomy duration as it's conducted in [24] and [25].

For instance, in [26] Abed proposes a hybrid approach combining classical intuitive sizing with more advanced numerical computation techniques. In this methodology, the intuitive method is used as a starting point to estimate the size of the PV generator and the battery storage system, before applying a more detailed optimization process. Although this approach improves technical reliability and economic performance, it still relies on a storage autonomy duration fixed a priori at one day, which does not necessarily guarantee an optimal solution and does not allow for an explicit consideration of battery aging.

Similarly, [20] Ali *et al.* (2023) combine an intuitive sizing approach with the PVsyst software to design standalone PV systems with battery storage intended to supply healthcare centers in several localities in Mali. A sensitivity analysis is conducted to assess the influence of storage autonomy duration – considered between one and three days on system size. The results show that both the peak power of the PV generator and the storage capacity are strongly dictated by the selected number of autonomy days, thereby highlighting the necessity of explicitly considering storage autonomy duration as a key optimization variable in the sizing process.

Based on these observations, the research hypothesis of this study is that the joint integration of an iterative sizing approach based on hourly time-series data, the explicit consideration of storage autonomy as an optimization variable, and a predictive battery aging model can significantly enhance both the technical reliability and economic viability of standalone PV systems. Our objective is to propose an iterative approach to optimize the conventional intuitive sizing of standalone PV systems with storage. This proposed iterative approach leverages hourly irradiance and consumption profiles while integrating a predictive battery aging model to enhance both technical reliability and economic accessibility.

To achieve this objective, an optimal system sizing model is first developed. Then, a case study is used to simulate the model using MATLAB, and finally, the simulation results are analyzed and discussed. Although the proposed methodology is general and can be applied to different geographical contexts, it is implemented and demonstrated in this study using real solar irradiation and temperature data from Zagtouli (Burkina Faso), together with a representative rural household load profile. Since PV system sizing strongly depends on both local solar resource variability and demand characteristics, the study is intentionally contextualized to reflect realistic operating conditions in Burkina Faso.

The main contributions of this study can be summarized as follows:

- The development of a fully iterative sizing methodology based on hourly time-series data of solar irradiation and load demand.
- The explicit consideration of storage autonomy as an optimization variable, rather than as a fixed design assumption.
- The integration of a predictive battery aging model (Rainflow counting combined with Miner's rule) directly into the techno-economic optimization framework.
- The implementation and validation of the proposed methodology using real measured climatic data from Zagtouli (Burkina Faso), ensuring realistic operating conditions.

MATERIALS AND METHODS

In this section, the methodology used to model and optimize the standalone PV system is presented. It begins with a description of the physical system, followed by the classical sizing

formulas and the modeling of global solar irradiance on tilted surfaces. Then, the modeling of system components, performance indicators, and battery aging is detailed, before presenting the iterative optimization approach.

Physical System

The physical electrical system to be sized is represented in **Figure 1**. It's a standalone PV system consisting of a PV generator, a battery bank, a charge controller, and a hybrid inverter. Optimally sizing such a system involves determining the optimal sizes of its main components (PV generator and battery bank) to best meet the user's energy demand while minimizing the cost of energy.

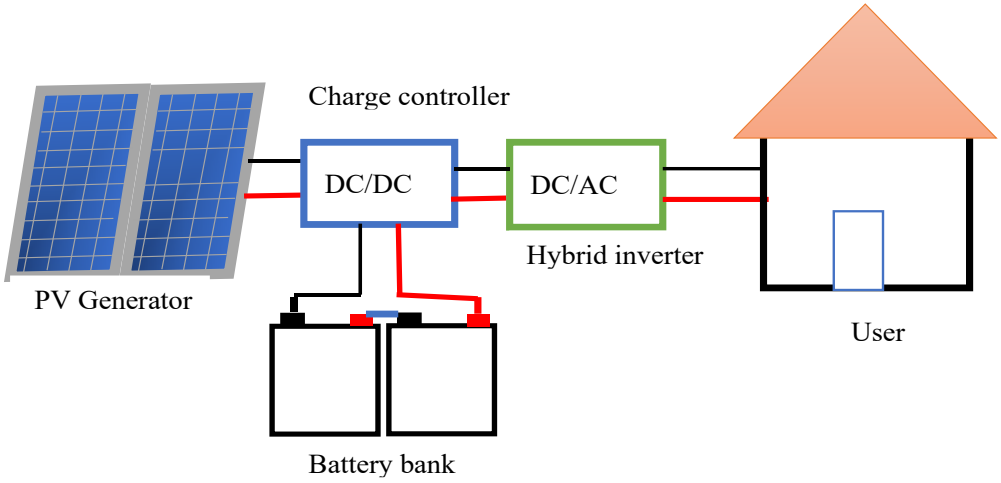

Figure 1. Physical system to size

Classical Sizing Formulas

The conventional intuitive method is based on simple formulas that consider only averaged values and involve intuitive choices for storage autonomy. Traditionally, the PV generator size P_{P} [W_p] and the battery storage capacity S_{BAT} [Ah] are respectively estimated using eq. (1) and eq. (2), as mentioned in [7]:.

$$P_{\mathrm{P}} = \frac{E_{\mathrm{D}} \times G_{\mathrm{R}}}{I_{\mathrm{D}} \times \eta_{\mathrm{g}}} \tag{1}$$

$$S_{\mathrm{BAT}} = \frac{E_{\mathrm{D}} \times N_{\mathrm{D}}}{U_{\mathrm{BAT}} \times DOD_{\mathrm{MAX}} \times \eta_{\mathrm{BAT}}} \tag{2}$$

where E_{D} [Wh/day] is the daily energy demand, G_{R} [W/m²] is the reference irradiance value (1000 W/m²), I_{D} [Wh/m²/day] is the average daily solar irradiation, η_{g} [%] is the overall efficiency of the PV generator, N_{D} [days] is the number of autonomy days, U_{BAT} [V] is the voltage across the battery bank, η_{BAT} [%] is the battery efficiency and DOD_{MAX} [%] is the maximum depth of discharge of the batteries.

Global Tilted Irradiance Modeling

The global solar irradiance measured on an inclined plane $G_{\mathrm{IT}}(t)$ [in W/m²] is expressed as the sum of the direct or beam solar irradiance $TBI(t)$, the diffuse component $TDI(t)$ from the sky dome and the fraction $TRI(t)$ reflected by the ground, as described by eq. (3). These three components are respectively given by eq. (5), eq. (4) and eq. (6).

In general, meteorological stations provide only the global irradiance measured on a horizontal plane $G_{\mathrm{HI}}(t)$ [in W/m²].

In this study, the irradiance received by photovoltaic modules tilted at an angle β is estimated from this horizontal measurement using the Erbs model presented in [27] for the direct – diffuse separation and the Hay–Davies transposition model also presented in [27] to reconstruct the global irradiance incident on the tilted surfaces.

$$G_{\mathrm{IT}}(t) = TBI(t) + TDI(t) + TRI(t) \tag{3}$$

$$TBI(t) = G_{\mathrm{HI}}(t) \times \left(1 - F_{\mathrm{d}}(t)\right) \times R_{\mathrm{g}}(t) \tag{4}$$

$$TDI(t) = G_{\mathrm{HI}}(t) \times F_{\mathrm{d}}(t) \times \left[A(t) \times R_{\mathrm{g}}(t) + \left(1 - A(t)\right) \times \left(\frac{1 + \cos(\beta)}{2}\right)\right] \tag{5}$$

$$TRI(t) = \rho \times G_{\mathrm{HI}}(t) \times \left(\frac{1 - \cos(\beta)}{2}\right) \tag{6}$$

where the hourly diffuse fraction $F_{\mathrm{d}}(t)$ of the horizontal global irradiance is given by eq. (7):

$$F_{\mathrm{d}}(t) = \frac{HDI(t)}{G_{\mathrm{HI}}(t)} = \begin{cases} 0.995 - 0.081 \times k \text{ if } k \leq 0.21 \\ 0.724 + 2.738 \times k - 8.32 \times k^2 + 4.967 \times k^3 \text{ if } 0.21 < k \leq 0.76 \\ 0.180 \text{ if } k > 0.76 \end{cases} \tag{7}$$

$R_{\mathrm{g}}(t)$ is a function of the atmospheric transmittance. It is also called geometric factor and can be found using eq. (8):

$$R_{\mathrm{g}}(t) = \frac{\cos(i)}{\sin(h)} = \frac{\cos(h)\cos(a_{\mathrm{s}} - a_{\mathrm{m}})\sin(\beta) + \sin(h)\cos(\beta)}{\cos(L)\cos(\delta)\cos(\omega) + \sin(L)\sin(\delta)} \tag{8}$$

$A(t)$ is the anisotropy index that is a function of the atmospheric transmittance for beam radiation and is given by eq. (9):

$$A(t) = \frac{HBI(t)}{G_0(t)} = \frac{G_{\mathrm{HI}}(t) \times \left(1 - F_{\mathrm{d}}(t)\right)}{G_0(t)} \tag{9}$$

where $G_{\mathrm{HI}}(t)$ [W/m²] is the global horizontal irradiance, $HBI(t)$ [W/m²] is the global horizontal direct or beam irradiance, $HDI(t)$ [W/m²] is the global horizontal direct or beam irradiance, and ρ is the ground reflectance constant that varies based on the surroundings of the tilted surface.

According to [28], the commonly used values for ground reflectance are ρ = 0.2 for hot and humid tropical locations, ρ = 0.5 for dry tropical locations, and ρ = 0.9 for snow-covered terrain. Here, β [°] denotes the tilt angle of the PV modules, h [°] the solar altitude, i [°] the incidence angle of the solar radiation, ω [°] is the hour angle, δ [°] is the declination angle, L [°] is the latitude of the installation site, a_{m} [°] is the PV module azimuth angle, and a_{s} [°] is the sun azimuth angle.

$k(t)$ is the clearness index and mathematically defined by eq. (10):

$$k(t) = \frac{G_{\mathrm{HI}}(t)}{G_0(t)} \tag{10}$$

where $G_0(t)$ [W/m²] is the extraterrestrial irradiance and given by eq. (11) as a function of the solar altitude h [°] and the day number of the year *N*. This irradiance varies by ±3.3% around the solar constant (1367 W/m²) due to the ellipticity of the Earth's orbit:

$$G_0(t) = 1367 \times \sin(h) \times (1 + 0.033 \times \cos(0.98 \times N)) \tag{11}$$

The evaluation of the tilted global irradiance model was performed using the coefficient of determination R^2 given by eq. (12), which indicates the proportion of the variability in measured data explained by the model, and the Root Mean Square Error (*RMSE*) given by eq. (13), which represents the typical average deviation between modeled and measured values in the same unit (W/m²):

$$R^2 = 1 - \frac{\sum_{t=1}^{8760}(G_{\mathrm{TI}}(t)measured - G_{\mathrm{TI}}(t)modeled)^2}{\sum_{t=1}^{8760}(G_{\mathrm{TI}}(t)measured - \overline{G_{\mathrm{TI}}measured})^2} \tag{12}$$

$$RMSE = \sqrt{\frac{1}{8760} \times \sum_{t=1}^{8760}(G_{\mathrm{TI}}(t)measured - G_{\mathrm{TI}}(t)modeled)^2} \tag{13}$$

where: $G_{\mathrm{TI}}(t)measured$ is the global tilted irradiance measured, $G_{\mathrm{TI}}(t)modeled$ is the global tilted irradiance modelled, and $\overline{G_{\mathrm{TI}}measured}$ is the annual average of the global tilted irradiance measured.

Physical System Components Modeling

In order to simulate the system behavior under operating conditions and optimaly size it, it's necessary to model its main components (PV generator and Battery bank). Thus, the PV generator is modeled by its instantaneous output power $P_{\mathrm{PV}}(t)$ [W] by equation eq. (14) as it's mentioned in [29]. It's mainly depended on the global tilted irradiance $G_{\mathrm{TI}}(t)$ [W/m²] receives on its surface inclined β [°] relative to the horizontal at each time t of the year at the installation site and the PV modules temperature $T_{\mathrm{mod}}(t)$ [°C] given by eq. (15):

$$P_{\mathrm{PV}}(t) = P_{\mathrm{P}} \times \frac{G_{\mathrm{TI}}(t)}{G_{\mathrm{R}}} \times F \times (1 - c \times (T_{\mathrm{mod}}(t) - T_{\mathrm{aR}})) \tag{14}$$

$$T_{\mathrm{mod}}(t) = T_{\mathrm{a}}(t) + \frac{G_{\mathrm{TI}}(t)}{G_{\mathrm{R}}} \times (T_{\mathrm{NOCT}} - T_{\mathrm{aR}}) \tag{15}$$

where P_{P} [W_p] is the peak power of the PV generator, G_{R} and T_{aR} are respectively reference irradiance and temperature values (1000 W/m² and 25 °C), F [%] is the soiling factor representing the power reduction due to dust (0.85), c is the temperature coefficient (0.386%/°C), $T_{\mathrm{a}}(t)$ is the instantaneous ambient temperature [°C], $G_{\mathrm{TI}}(t)$ is the instantaneous global tilted irradiance [W/m²], T_{NOCT} is module temperature at 800 W/m² irradiance and 25 °C ambient temperature.

When it's come to the Batteries Bank, it is modeled by its storage capacity S_{BAT} [Ah] and state of charge *SOC* [Wh]. To optimize the battery storage capacity which is a key design parameter, eq. (2) has been reformulated as expressed in eq. (16) by replacing the daily energy requirement E_{D} [Wh/days] with the average hourly consumption E_{MH} [Wh/h] given by eq. (17) and the number of autonomy days N_{D} [days] with the number of autonomy hours N_{H} [h]:

$$S_{\mathrm{BAT}} = \frac{E_{\mathrm{MH}} \times N_{\mathrm{H}}}{U_{\mathrm{BAT}} \times DOD_{\mathrm{MAX}} \times \eta_{\mathrm{BAT}}} \tag{16}$$

$$E_{\mathrm{MH}} = \frac{\sum_{t=1}^{24}(P_{\mathrm{CH}}(t) \times \Delta t)}{t_{\mathrm{MAX}}} \tag{17}$$

where t_{MAX} [h] corresponds to the number of hours with non-zero power demand.

The state of charge $SOC(t)$ [Wh] is given as a function of the surplus or deficit (positive for surplus and negative for deficit) of production $\Delta P(t)$ [W] and the battery efficiency η_{BAT} [%] by eq. (18):

$$SOC(t) = SOC(t-1) + \Delta P(t) \times \Delta t \times \eta_{\mathrm{BAT}} \tag{18}$$

where Δt [h] is simulation time step. In this study, a time step of 1h is considered.

The production deficit or excess at each time t $\Delta P(t)$ [W] is given by eq. (19):

$$\Delta P(t) = P_{\mathrm{PV}}(t) \times \eta_{\mathrm{Reg}} - P_{\mathrm{CH}}(t) \times \frac{1}{\eta_{\mathrm{Ond}}} \tag{19}$$

where η_{Reg} [%] and η_{Ond} [%] are the efficiencies of the charge controller and the inverter, respectively. $P_{\mathrm{CH}}(t)$ [W] is the load power at each time *t* of the year.

The state of charge is constrained to evolve within a specific range to avoid rapidly degrading the batteries due to overcharging or excessive discharging, as shown in the system of eq. (20):

$$\begin{cases} SOC_{\mathrm{MIN}} \leq SOC(t) \leq SOC_{\mathrm{MAX}} \\ SOC_{\mathrm{MAX}} = P \times S_{\mathrm{BAT}} \\ SOC_{\mathrm{MIN}} = (1 - DOD_{\mathrm{MAX}}) \times SOC_{\mathrm{MAX}} \end{cases} \tag{20}$$

where SOC_{MAX} [Wh] is the maximum state of charge of the battery, SOC_{MIN} [Wh] is the minimum state of charge of the battery, P [%] is the percentage term representing the maximum energy level not to be exceeded in the batteries during charging and DOD_{MAX} [%] is the maximum depth of discharge of the battery.

Indicators Performance Modeling

The technical and economic performance of the system is evaluated using respectively the Loss of Power Supply Probability (*LPSP*) and the Levelized Cost of Energy (*LCOE*). The *LPSP* [%] is the indicator generally used to assess or measure the technical reliability of electricity generation systems **[30]**. It is expressed here by eq. (21):

$$LPSP = \frac{\sum_{t=1}^{8760} LPS(t)}{\sum_{t=1}^{8760}(P_{\mathrm{CH}}(t) \times \Delta t)} \tag{21}$$

where $LPS(t)$ [Wh] corresponds to the energy deficit at each hour of the year. It is expressed by eq. (22):

$$LPS(t) = (-\Delta P) \times \Delta t - (SOC(t-1) - SOC_{\text{MIN}}) \tag{22}$$

where ΔP [W] is previously given by eq. (19). It corresponds to the difference between the power supplied by the PV generator and the power demanded by the user's load. The $LCOE$ [EUR/kWh] is the indicator most used to assess the cost per kWh produced by the system or to measure the economic feasibility of electricity generation systems [30]. It is expressed here by eq. (23):

$$LCOE = \frac{NPV}{\sum_{t=1}^{8760}(P_{\text{PV}}(t) \times \Delta t)} \times CRF \tag{23}$$

where NPV [EUR] is the Net Present Value, defined by eq. (24), taking into account the total initial investment cost C_{IT} [EUR], the operation and maintenance costs C_{OM} [EUR] which correspond to a certain percentage m [%] of the investment cost and the replacement costs C_{R} [EUR] of certain component respectively given by eq. (25), eq. (26) and eq. (27). CRF [%] is the Capital Recovery Factor which is precisely the annualization factor used to convert a Net Present Value (NPV) into an equivalent annual cost:

$$NPV = C_{\text{IT}} + C_{\text{OM}} + C_{\text{R}} \tag{24}$$

$$C_{\text{IT}} = C_{\text{Smod}} \times P_{\text{P}} + C_{\text{SBAT}} \times S_{\text{BAT}} + C_{\text{Ond}} + C_{\text{Reg}} + C_{\text{SUP-INST}} \tag{25}$$

$$C_{\text{OM=}} C_{\text{IT}} \times m \times F_{\text{a}} \tag{26}$$

$$C_{\text{R}} = \sum_{j} C_{(\text{IT})_j} \times F_{\text{a}_j} \tag{27}$$

where C_{Smod} [EUR/W_p] and C_{SBAT} [EUR/W_p] correspond to the specific costs of a module a battery, respectively. C_{Reg} [EUR] and C_{Ond} [EUR] correspond to the costs of the charge controller and the inverter, respectively. $C_{\text{SUP-INST}}$ [EUR] represents the cost of the mounting structures and the installation of the system and is taken here as 40% of the purchase cost of the PV generator modules and batteries bank. CRF [%], F_{a} [%] andF_{a_j} [%] correspond to the annualization factor, the overall discount factor for maintenance costs, and the discount factor for the replacement cost of each component j that needs to be replaced in the system, respectively. They are respectively given by eq. (28), eq. (29), and eq. (30) [30]:

$$CRF = \frac{a_{\text{r}}(1-a_{\text{r}})^{D_{\text{S}}}}{(1+a_{\text{r}})^{D_{\text{S}}} - 1} \tag{28}$$

$$F_{\text{a}} = \begin{cases} \left(\frac{1+i}{a_{\text{r}}-i}\right) \times \left[1 - \left(\frac{1+i}{a_{\text{r}}-i}\right)^{D_{\text{S}}}\right] \text{ if } a_{\text{r}} \neq i \\ D_{\text{S}} \text{ if } a_{\text{r}} = i \end{cases} \tag{29}$$

$$F_{a_j} = \sum_{k=1}^{N_{R_j}} \left(\frac{1+i}{1+a_r}\right)^{\frac{k}{N_{R_j}+1}} \quad (30)$$

where D_S [years] is the lifetime of the system, a_r [%] is the real interest rate, i [%] is the inflation rate and k is the k-th replacement.

N_{R_j} is the number of replacements of each component j defined by eq. (31):

$$N_{R_j} = \left(\frac{D_S}{D_j}\right) 1 \quad (31)$$

where D_j [years] is the lifetime of each component j and D_S [years] is the system lifetime.

Batteries Bank Aging Modeling

The lifetime of the batteries is a parameter that plays a role in the economic analysis of autonomous PV systems with storage. However, designers of these systems often use the battery lifetime provided by the manufacturer for a specific use where the charge-discharge cycles are regular. In autonomous PV systems with storage, the cycling of the storage is not regular due to the fluctuation of solar resource.

To account for this aspect in the sizing of these systems, a battery aging calculation model already proposed in [31] and based on manufacturer data has been integrated into the iterative approach developed in this study to predict the storage lifetime.

Thus, to evaluate the battery lifetime, the process followed is presented in Figure 2. In this process, the state of charge profile of the battery obtained from the system simulation is first subjected to the Rainflow cycle counting algorithm, which converts it into a series of depth of discharge values with j going from 1 to n. After that, the Miner's rule is applied initially to assess the total fraction of damage T_{VA} [%] expressed by eq. (32), also called the annual aging rate. The battery lifetime is finally deduced in years from the annual aging rate using eq. (33) below.

$$T_{VA} = 100 \times \sum_{j=1}^{n} \frac{1}{N_{C_j}(DOD_j)} \quad (32)$$

$$D_{BAT} = 100 \times (T_{VA})^{-1} \quad (33)$$

where n corresponds to the cycle number counted and $N_{C_j}(DOD_j)$ is the number of cycles associated with depth of discharge number j. This number is obtained by using the fitting power law equation (eq. (34)) below with two coefficients (a and b). These coefficients depend on the type of battery technology meaning that this fitting model is unique for every battery and is derived based on information from the manufacturer datasheet. For the study-case battery the fitted model is shown with a red line in Figure 7a.

$$N_{C_j}(DOD_j) = a(DOD_j)^b \quad (34)$$

For example, if the aging rate is 25%, then the battery lifetime is deduced to be 4 years. Miner's rule states that for a given depth of discharge, the damage caused to the battery by a cycle is equal to the inverse of the number of cycles associated with that depth of discharge.

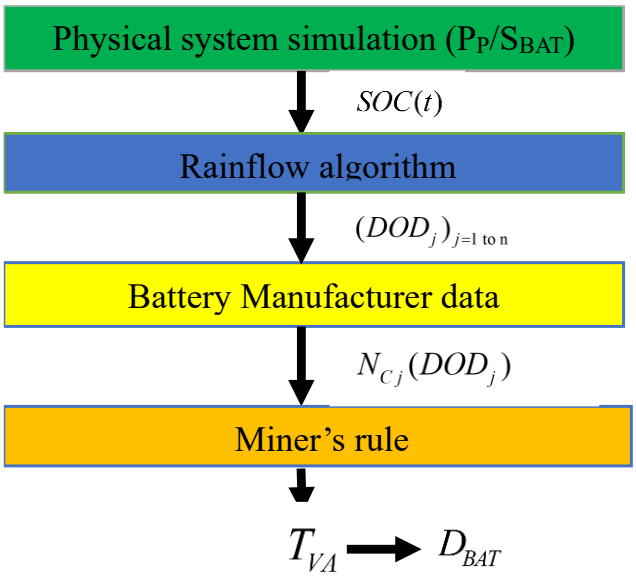

Figure 2. Batteries bank aging calculation model

Optimization Problem and Iterative Algorithm

Based on the mathematical models of the main components of the physical system, performance indicators, and storage aging, the optimization problem for sizing is formulated according to the system of eq. (33) below. The problem thus consists of finding a peak power P_{P} [WP] of the PV generator and storage autonomy N_{H} [h] which are capable of covering the user's needs as widely as possible and at the lowest cost.

$$\boldsymbol{S}: \begin{cases} Min\ LCOE(P_{\mathrm{P}}, N_{\mathrm{H}}) \\ LPSP(P_{\mathrm{P}}, N_{\mathrm{H}}) \leq LPSP_{\mathrm{MAX}} \\ SOC_{\mathrm{MIN}} \leq SOC(t) \leq SOC_{\mathrm{MAX}} \\ P_{\mathrm{P_{MIN}}} \leq P_{\mathrm{P}} \leq P_{\mathrm{P_{MAX}}} \\ 1 \leq N_{\mathrm{H}} \leq N_{\mathrm{H_{MAX}}} \end{cases} \tag{35}$$

To solve the previously defined optimization problem, an iterative algorithm developed in the MATLAB environment was implemented. The flowchart presented in **Figure 3** illustrates the overall structure of the proposed optimization methodology. The algorithm begins by importing the weather and load data, the battery aging characteristics provided by the manufacturer, the techno-economic parameters and unit costs and the optimization constraints. For each considered number of autonomy hours, N_{H} the peak power of the PV generator $P_{\mathrm{P}}$is iteratively increased from $P_{\mathrm{P_{MIN}}}$to $P_{\mathrm{P_{MAX}}}$with a predefined step ΔP_{P}.

For each configuration (N_{H},P_{P}), an hourly energy balance is performed over one full year (8760 hours). At each time step $\Delta P(t)$ which corresponds to de difference between the PV generator production and the load demand is evaluated. The battery state of charge (SOC) is updated depending on whether the system is in charging or discharging mode, while strictly enforcing the operational limits SOC_{MIN} and SOC_{MAX} Whenever the battery reaches its lower bound and all the load is not met, the unmet load is quantified through the instantaneous loss of power supply $LPS(t)$. After completing the annual simulation, the Loss of Power Supply Probability ($LPSP$) is calculated. The algorithm then evaluates and stores the battery lifetime using the rainflow cycle counting method, the total annual energy produced and the Levelized Cost of Energy ($LCOE$). The process continues until the maximum autonomy hours $N_{\mathrm{H_{MAX}}}$ is reached.

Finally, only configurations whose $LPSP$ is below to the $LPSP_{\mathrm{MAX}}$ ($LPSP \leq LPSP_{\mathrm{MAX}}$) are considered technically feasible. The configuration offering the best compromise between system reliability (low LPSP) and economic performance (minimum $LCOE$), ensuring both technical feasibility and cost-effectiveness is selected among all feasible configurations as the optimal solution.

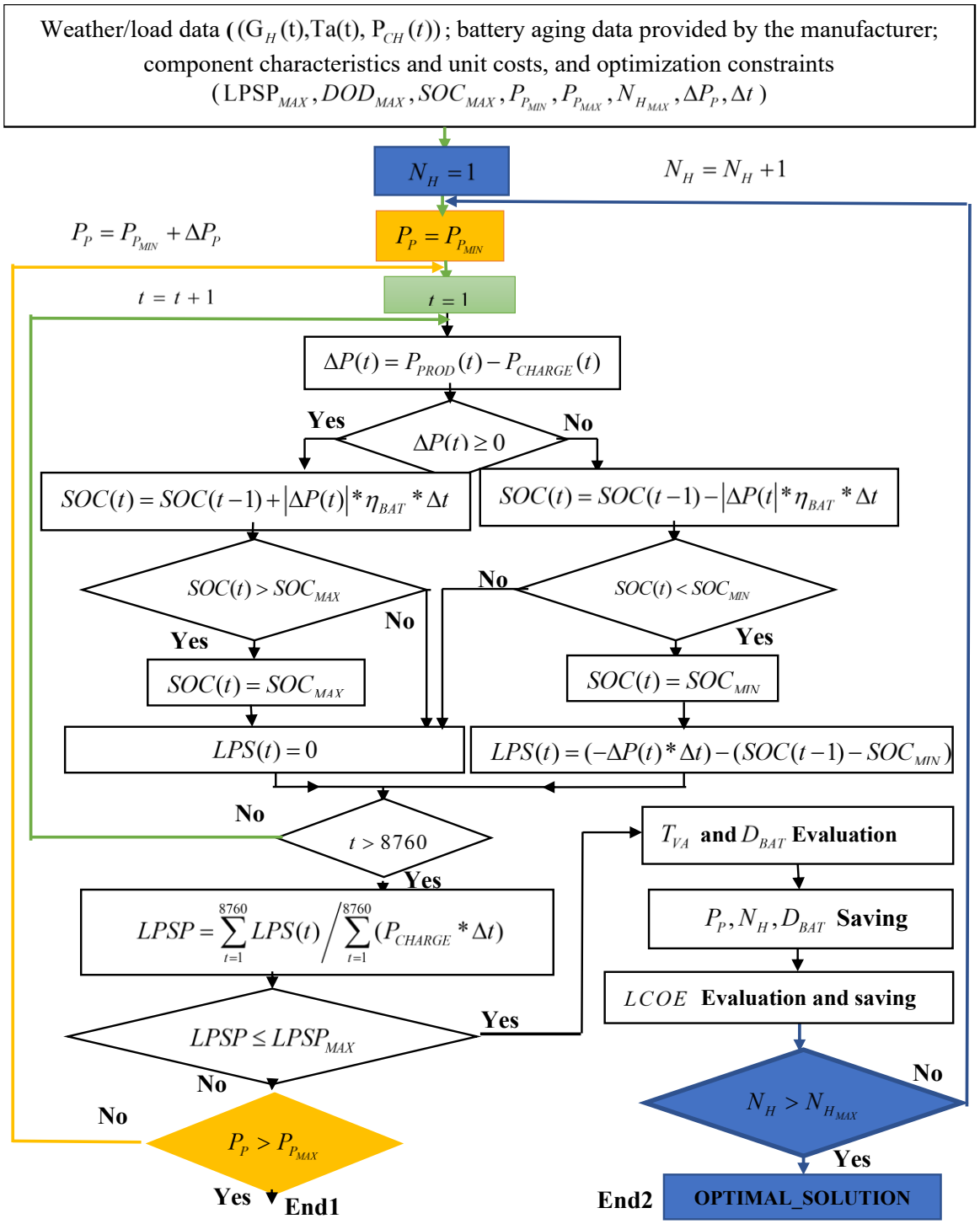

Figure 3. Flowchart of the Sizing Program

RESULTS AND DISCUSSION

The proposed iterative sizing approach is applied to a real case study to evaluate its effectiveness in meeting technical and economic objectives. The following subsections describe the case study data, modeling results, and their discussion.

Case Study

To apply the iterative approach developed in this study, hourly profiles of solar irradiation, ambient temperature, and household consumption from a peri-urban neighborhood of Ouagadougou (Zagtouli) illustrated in **Figure 4** were used. The meteorological data come from the weather station installed in this locality of Burkina Faso. The consumption curve presented in **Figure 4c** shows two peaks: one at 5 AM and another at 8 PM. The solar irradiation and ambient temperature profiles fluctuate throughout the year, illustrating the variation in solar resources and their influence on temperature. The technical and financial characteristics of the system components, as well as their lifespan, are listed in **Table 1**. The interest and inflation rates used are the same as those in the *LCOE* calculation in **[32]**. The photovoltaic modules used are 265 W_p panels assembled by Faso Energy, a Burkinabe company specializing in photovoltaic cell assembly. These panels are oriented due south with a 12° tilt, corresponding to the latitude of Ouagadougou. **Table 2** presents the number of battery cycles depending on the depth of discharge for a specific application. These data were provided by the manufacturer. **Table 3** specifies the technical constraints adopted in the system design.

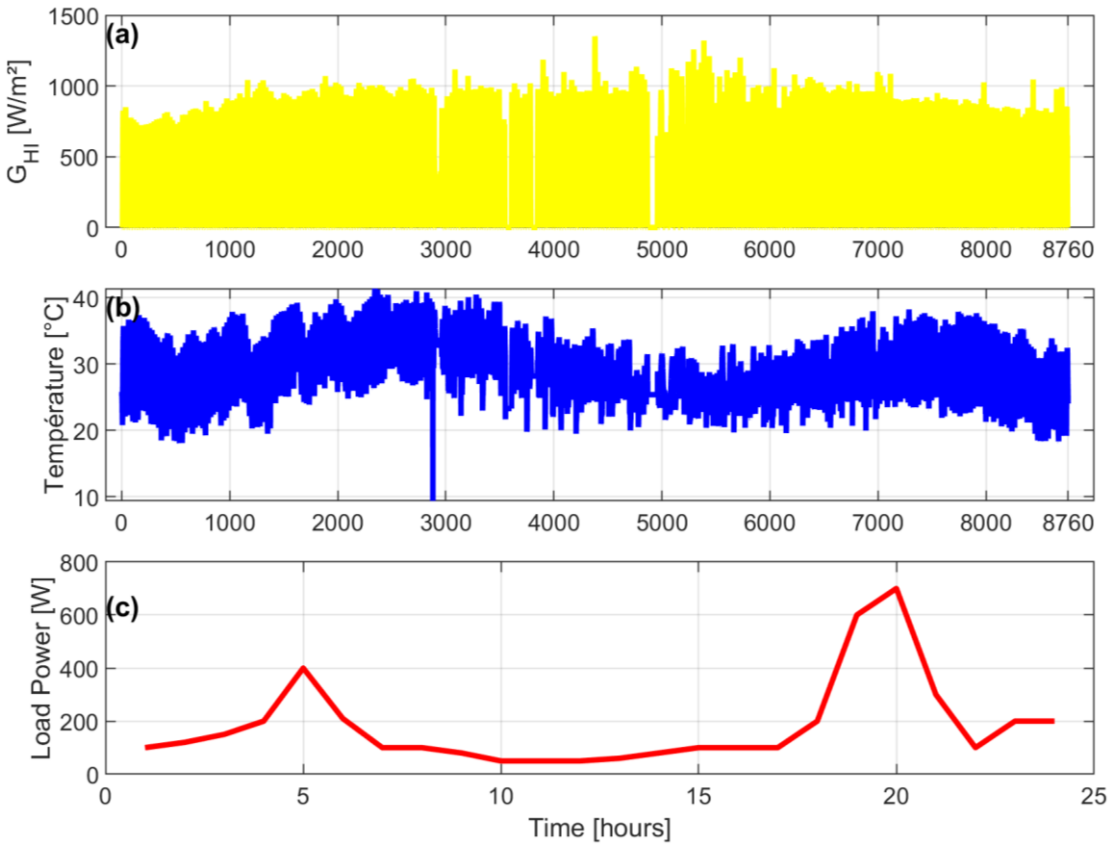

Figure 4. (a) Hourly profile of irradiance on a horizontal plane; (b) Hourly profile of ambient temperature; (c) Hourly profile of household consumption

Table 1. Characteristics, costs, and lifespan of the system components

Components/system	Characteristics	Costs	Lifespan [years]	Interest rate [%]	Inflation rate [%]
PV Poly module (Faso Energy)	12V/265W_P	0.40 EUR/W_p	20	8	3
AGM Battery (Victron Technology)	12V/60Ah Efficiency=85%	0.06 EUR/Wh	To predict	----	-----
Charge Controler	48V/30A	94.98 EUR	10	----	-----
Phoenix hybrid Inverter	48V/1200W 230V AC /50HZ	474.72 EUR	10	----	-----
System	-----	---	20	----	----

Table 2. Number of regular cycles based on the maximum depth of discharge of the AGM battery

DOD [%]	30	50	60	80
Number of regular cycles given by the Manufacturer [cycles]	1800	750	600	500

Table 3.Technical optimization constraints

$LPSP_{MAX}$ [%]	DOD_{MAX} [%]	SOC_{MAX} [%]	$P_{P_{MAX}}$ [W_p]	$P_{P_{MIN}}$ [Wp]	$N_{H_{MIN}}$ [h]	ΔP_P [W_p]
10	70	90	26500	265	48	265

After simulating the sizing model using the input parameters previously defined in **Figure 4** and **Table 1**, **Table 2**, and **Table 3**, the following results were obtained:

Global Irradiance on Tilted Surface

The **Figure 5** presents the evolution of the measured global horizontal irradiance (*GHI*), the measured global tilted irradiance (measured *GTI*), and the modeled tilted irradiance (*GTI* model) over two consecutive days of the year. A typical daily solar cycle is observed, with a rapid increase in the morning, a peak of about 1000 W/m² near solar noon, and a symmetric decline in the afternoon.

The measured tilted irradiance remains higher than the horizontal irradiance during daylight hours, as expected, since tilted PV modules intercept a larger portion of the direct solar radiation.

The modeled tilted irradiance obtained using the Erbs and Hay–Davies methods (orange curve), closely matches the measurements, accurately reproducing both the amplitude and the daily pattern.

A coefficient of determination (R^2) of 0.96, indicating that 96 % of the variability in measured irradiance is explained by the model, and an *RMSE* of 65.30 W/m^2, representing the typical deviation between modeled and measured values, confirm the model's reliability in estimating tilted-plane irradiance from horizontal data. Minor deviations, particularly near solar noon, mainly reflect atmospheric variability or measurement uncertainties.

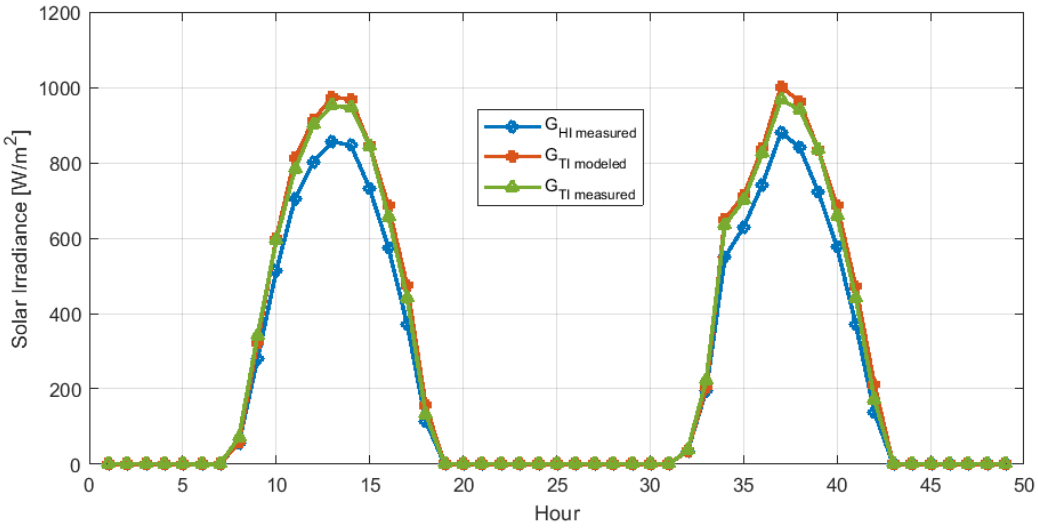

Figure 5. Measured and modeled global irradiance on a tilted surface over two consecutive days

Influence of Autonomy on PV Generator Size, *LPSP*, *LCOE* and Storage Lifetime

Figure 6a illustrates the PV generator size and LPSP as a function of battery autonomy. For an autonomy of 1 to 13 hours, the PV generator size remains fixed at 25,600 Wp, while the LPSP decreases linearly from 70% to 11%. This means that with an autonomy of 13 hours or less, it is impossible to achieve an LPSP of 10% or lower, regardless of the PV generator used. In this range (1h to13 h of autonomy), the optimization algorithm progressively increases the PV generator size up to its maximum allowable value (26.5 kWp) in an attempt to satisfy the LPSP constraint. However, due to the very limited storage capacity associated with low autonomy levels, most of the daytime PV production cannot be effectively stored and is therefore curtailed. As a result, the nighttime household demand remains largely unmet, and the LPSP constraint cannot be achieved even with the maximum PV generator size. Between 13 and 16 hours, the generator size drops rapidly from 26,500 Wp to 1,060 Wp and remains constant beyond that, while the LPSP decreases from 11% to 9.35%, then declines more slowly. From 13 h of autonomy onward, the storage capacity becomes sufficiently large to cover a significant share of the household's nighttime demand. This allows the optimization algorithm to drastically reduce the PV generator size while still satisfying the LPSP $\leq$ 10% constraint. Consequently, the sharp decrease in PV generator size observed in this interval reflects a transition from a PV-dominated strategy to a storage-driven reliability improvement. An autonomy beyond 17 hours slightly reduces the LPSP but significantly increases storage size, impacting the LCOE. Thus, a minimum autonomy of 17 hours and a PV generator of 1,060 Wp are required to meet 90% of the household's annual energy demand. This region therefore corresponds to an optimal trade-off, where a relatively moderate storage autonomy (around 16–17 h) enables high supply reliability with a minimal PV generator size, thereby defining a techno-economic "sweet spot" for system design.

Figure 6b shows the curves of LCOE and storage lifespan as a function of storage autonomy. For an autonomy of 13 hours or less, the LCOE (0.05 EUR) and storage lifespan (1.80 years) remain constant due to the stable size of the PV generator and the low storage capacity. However, this autonomy does not meet the 10% LPSP threshold. Between 13 and 16 hours, the LCOE increases rapidly (0.05 to 0.20 EUR), while the storage lifespan rises to 2 years. In this interval, the rapid increase in LCOE is mainly driven by the growth of storage capacity, which becomes the dominant cost component of the system, while the PV generator size is significantly reduced. Beyond 16 hours, the storage lifespan grows linearly, and the LCOE fluctuates, likely due to variations in the number of battery replacements required for the storage system. Beyond 16 h of autonomy, further increases in storage capacity do not reduce the PV generator size any further, but they continue to increase the investment and

replacement costs of the battery system. The observed LCOE fluctuations are therefore mainly associated with variations in the predicted storage lifetime and, consequently, in the number of battery replacements over the project lifetime.

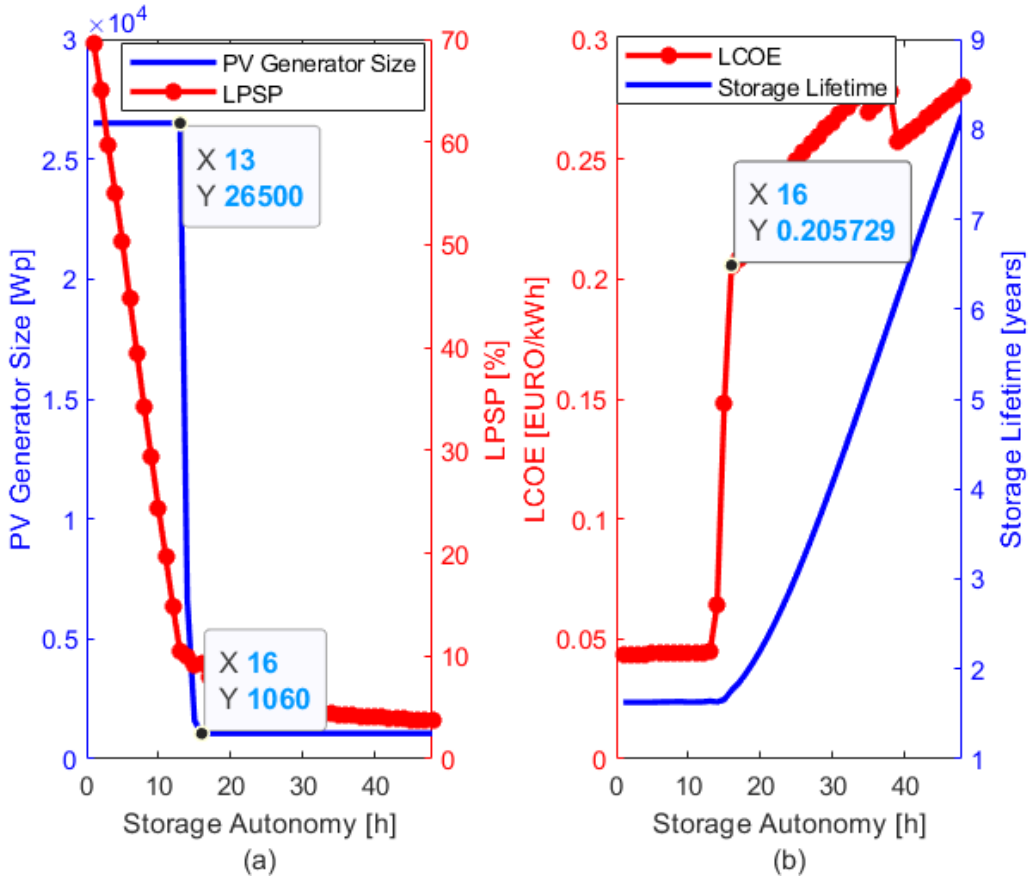

Figure 6. (a) PV Generator and *LPSP* evolution as a function of storage autonomy; (b) *LCOE* and Battery lifetime evolution as a function of storage autonomy

Storage Lifetime Associated with the Optimal Configuration

In order to estimate the storage lifetime associated with the optimal configuration, a cycle-based aging methodology was adopted. This approach combines the manufacturer's cycle-life data, the simulated annual *SOC* profile, and a cycle counting procedure based on the Rainflow algorithm. The overall objective is to quantify the cumulative battery degradation under real operating conditions.

Figure 7a presents the aging curve of the AGM batteries used, obtained by fitting the data from manufacturer (**Table 2**) using MATLAB. This curve makes it possible to determine the number of regular cycles for any given Depth of Discharge (*DOD*). This aging model constitutes the reference framework for evaluating battery degradation once the actual operating cycles are identified from the simulated *SOC* profile. For the fit power law model used, the estimated coefficients are a=3.128×10 and b=−1.519. The goodness-of-fit indicators confirm the adequacy of the selected model, with a coefficient of determination R^2 and a root mean square error *RMSE*=87.74 cycles. The high R^2 value indicates that more than 98% of the variability in the manufacturer's cycle-life data is explained by the fitted function.

Figure 7b now presents the state-of-charge (*SOC*) profile of the storage from the optimal configuration simulation, which ranges between 90% and 27% and complies with the defined storage management strategy. This *SOC* profile represents the real operating conditions of the battery over one year and serves as the input signal for the cycle counting analysis.

Figure 7c classifies the cycles by amplitude or *DOD* using the Rainflow algorithm. Based on the *SOC* profile shown in Figure 7b, the algorithm identifies 378 cycles. Each identified cycle is characterized by its amplitude (*DOD*), which allows associating it with the corresponding allowable number of cycles derived from the aging curve shown in Figure 7a. The cumulative damage is then calculated using Miner's rule, which assumes that the total degradation corresponds to the linear accumulation of partial damages induced by each cycle. When the accumulated damage reaches unity, the battery is considered to have reached its end of life. Based on this approach, the storage lifetime in the optimal configuration is estimated at approximately 2 years. This relatively short lifetime highlights the significant impact of the cycling profile and storage autonomy on battery degradation, confirming the strong coupling between reliability requirements and economic performance.

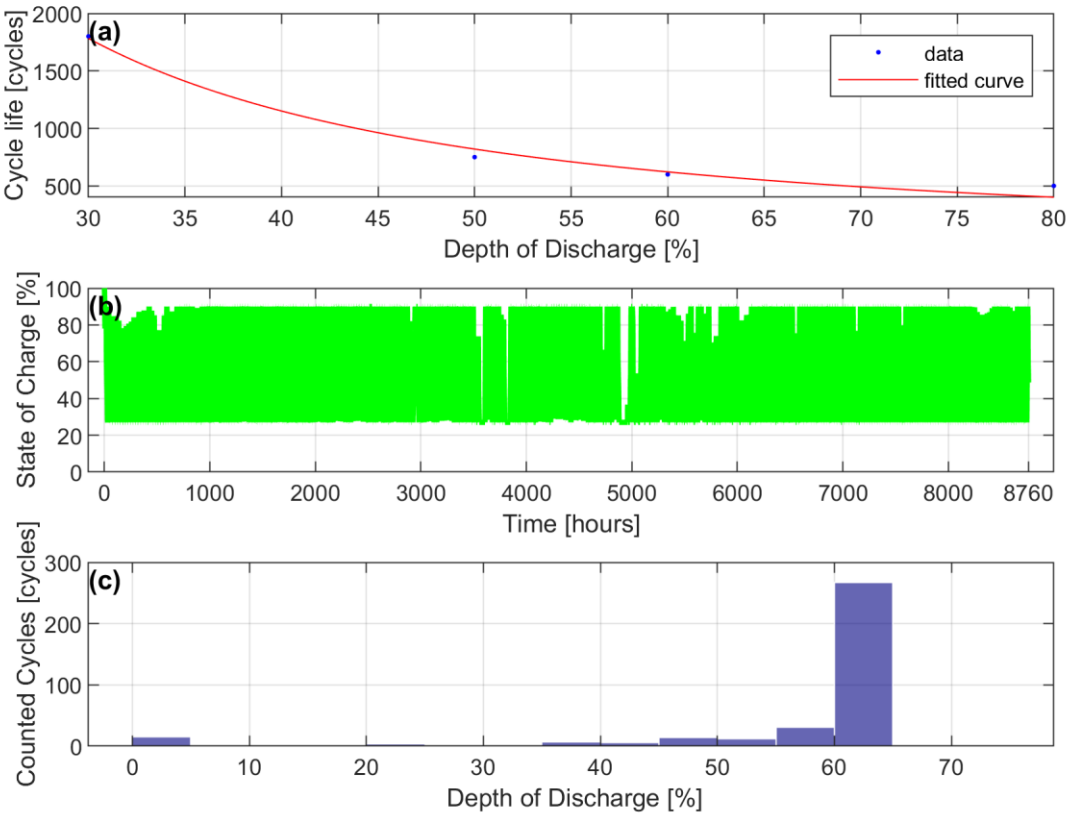

Figure 7. (a) Battery cycle life as a function of Depth of Discharge (*DOD*) based on manufacturer data and fitted aging model; (b) Battery Annual hourly State of Charge; (c) Distribution of cycle Depth of Discharge obtained using the Rainflow counting algorithm

Comparison between the Optimal Solution and the Conventional Solution

In the conventional method, the PV generator size is calculated using the average daily energy demand (4500 Wh), obtained by summing the hourly load over one day, the average daily solar irradiation at the Zagtouli site (5 kWh/m²/day), and an overall system efficiency of 0.7. This global efficiency results from the product of the charge controller efficiency (85%), inverter efficiency (90%), and dust-related losses (85%).

This simplified sizing approach relies on averaged quantities and does not explicitly consider the hourly interaction between PV production, storage operation, and load demand during the design phase. The storage capacity is determined assuming a fixed autonomy of one day, a battery bank voltage of 48 V, a battery efficiency of 85%, and a maximum depth of discharge (*DOD*) of 70%, as commonly adopted in conventional rural electrification practices.

To allow a fair comparison with the proposed approach, the conventional configuration was subsequently simulated under real hourly operating conditions using the same load profile and solar resource data. This simulation shows that the conventional solution achieves a reliability level comparable to that of the optimized configuration, with an *LPSP* of 9.02%, while the optimized solution yields an *LPSP* of 9.35%.

Despite these similar reliability levels, significant differences are observed in terms of economic performance. As shown in **Table 4**, the optimized configuration obtained from the proposed iterative optimization procedure consists of a PV generator size of 1060 W_p and 16 hours of storage autonomy, corresponding to a storage capacity of 100.60 Ah and an *LCOE* of 0.20 EUR/kWh.

When comparing both approaches, a 35.92% reduction in storage capacity is achieved with the optimized configuration, leading to a corresponding 37.50% reduction in *LCOE*. This indicates that the proposed method identifies a more cost-effective solution for nearly identical reliability levels.

The main difference between the two approaches therefore lies not in the achieved reliability, but in the sizing philosophy. The proposed optimization explicitly accounts for hourly system dynamics, storage aging, and economic trade-offs during the design stage, whereas the conventional method relies on fixed autonomy assumptions and averaged indicators. As a result, the optimized approach ensures a better compromise between economic performance and reliability while preserving the required comfort level of electricity supply.

Table 4. Comparison of the two-sizing solution provided by the conventional intuitive method and the iterative approach proposed in this study

Method	E_D [Wh/day]	P_P [W_p]	N_D [days] or N_H [h]	t_{MAX} [h]	S_{BAT} [Ah]	D_{BAT} [years]	$LPSP$ [%]	$LCOE$ [EUR /kWh]
Conventional Intuitive	4500	1125	1 day	---	157	2	9.35	0.32
Proposed approch	4500	1060	16 h	24	100.6	2	9.02	0.20

CONCLUSION

In this study, an iterative optimal sizing approach for a standalone PV system with battery storage, integrating a predictive model for battery aging, was first presented. This approach ensures a coherent coupling between system reliability, storage degradation under real operating conditions, and long-term economic evaluation, thereby avoiding the use of fixed or manufacturer-based lifetime assumptions in the *LCOE* calculation.

The approach was then applied in a case study to a household consumption profile in a peri-urban neighborhood of Ouagadougou, Burkina Faso. Measured meteorological data on a horizontal plane were used to determine the optimal system configuration capable of meeting at least 90% of the household's energy demand. With a typical daily consumption of 4.5 kWh, the minimum required sizes for the PV generator and battery bank to achieve this target are 1060 W_p and 100.60 Ah, respectively, resulting in a minimum energy cost of 0.20 EUR/kWh. The storage autonomy and lifespan obtained are 16 hours and 2 years, respectively.

Comparison with the conventional intuitive approach, still widely used today, shows that the proposed iterative method not only predicts battery lifespan within the system but also significantly reduces storage size and, consequently, the system's *LCOE*.

Although the case study focuses on Burkina Faso, the proposed methodology is general and can be applied to other geographical contexts, since system sizing fundamentally depends on local solar resource variability and load characteristics.

ACKNOWLEDGMENTS

This work was supported by the Regional Scholarship and Innovation Fund (RSIF) under the Partnership for Skills in Applied Sciences, Engineering, and Technology (PASET) Initiative. The authors thank the International Centre of Insect Physiology and Ecology (ICIPE) for managing the RSIF fund.

REFERENCES

1. UN Department of Economic and Social Affairs, Goal 7 | Ensure access to affordable, reliable, sustainable and modern energy for all, https://sdgs.un.org/goals/goal7, [Accessed: Dec. 07, 2025].
2. N. Schöne, E. Timofeeva, and B. Heinz, "Sustainable Development Goal Indicators as the Foundation for a Holistic Impact Assessment of Access-to-Energy Projects," *Journal of Sustainable Development of Energy, Water and Environment Systems*, Vol. 10, No. 2, 2022, https://doi.org/10.13044/J.SDEWES.D9.0400.
3. International Energy Agency, World Energy Outlook 2024 – Analysis, https://www.iea.org/reports/world-energy-outlook-2024, [Accessed: Dec. 07, 2025].
4. J. Schulte, J. Figgener, P. Woerner, H. Broering, and D. Uwe Sauer, Forecast-based charging strategy to prolong the lifetime of lithium-ion batteries in standalone PV battery systems in Sub-Saharan Africa, *Solar Energy*, Vol. 258, pp 130–142, 2023, https://doi.org/10.1016/J.SOLENER.2023.03.029.
5. F. Egli, C. Agutu, B. Steffen, and T. S. Schmidt, The cost of electrifying all households in 40 Sub-Saharan African countries by 2030, *Nature Communications,* Vol. 14, No. 1, 5066, 2023, https://doi.org/10.1038/s41467-023-40612-3.
6. N. B. Onyeanusi, Energy Access Implications for Unserved Communities in Sub-Saharan Africa: Challenges and Opportunities, *World Sustainability Series*, Vol. Part F571, pp 165–181, 2025, https://doi.org/10.1007/978-3-031-87043-9_9.
7. J. G. Kafando, D. Yamegueu, and E. T. Houdji, Review on sizing and management of stand-alone PV/WIND systems with storage, Vol. 10, No. 18, e38080, 2024, https://doi.org/10.1016/j.heliyon.2024.e38080.
8. T. Khatib, I. A. Ibrahim, and A. Mohamed, A review on sizing methodologies of photovoltaic array and storage battery in a standalone photovoltaic system, *Energy Convers. Manag.*, Vol. 120, pp 430–448, 2016, https://doi.org/10.1016/j.enconman.2016.05.011.
9. F. A. Alturki and E. M. Awwad, Sizing and Cost Minimization of Standalone Hybrid WT/PV/Biomass/Pump-Hydro Storage-Based Energy Systems, *Energies,* Vol. 14, No. 2, 2021, https://doi.org/10.3390/en14020489.
10. I. D. Sara, N. Rosmin, M. Bahi, and M. D. M. Zulkepli, DESIGN AND SIZING OF STAND-ALONE PHOTOVOLTAIC SYSTEMS FOR REMOTE AREAS, *Journal of Energy and Safety Technology*, Vol. 7, No. 2, pp 130–141, 2024, https://doi.org/10.11113/jest.v7.187.
11. M. Sidrach-de-Cardona and L. M. López, Study of the Aging of a Lead–Acid Battery Bank in a Multi-Source Hybrid System, *Electrical Engineering Symposium,* Cachan, France, Jul 2014, https://hal.archives-ouvertes.fr/hal-01065201, [Accessed: Dec. 07, 2025].
12. H. M. Ridha, C. Gomes, H. Hizam, M. Ahmadipour, D. H. Muhsen, and S. Ethaib, Optimum design of a standalone solar photovoltaic system based on novel integration of iterative-PESA-II and AHP-VIKOR Methods, *Processes*, Vol. 8, No. 3, 2020, https://doi.org/10.3390/PR8030367.

13. B. Li, Z. Liu, Y. Wu, P. Wang, R. Liu, and L. Zhang, Review on photovoltaic with battery energy storage system for power supply to buildings: Challenges and opportunities, *J. Energy Storage*, Vol. 61, p. 106763, 2023, https://doi.org/10.1016/j.est.2023.106763.
14. A. Mielcarek, B. Ceran, and J. Jurasz, The Impact of Degradation of PV/Battery-Independent System Components on Technical and Economic Indicators and Sizing Process, *Energies,* Vol. 16., 2023, https://doi.org/10.3390/en16186642.
15. M. Jiang, W. Zhang, W. Jiang, and H. Zhang, A Review of Optimization Models for Battery Sizing in Utility-scale Photovoltaic Power Plants, *Energy Proceedings*, 2025, https://doi.org/10.46855/energy-proceedings-11752.
16. M. Kouihi, M. Moutchou, and A. A. Elmahjoub, Sizing optimization of a standalone PV/wind hybrid energy system with battery storage using a genetic algorithm, *International Journal of Power Electronics and Drive Systems*, Vol. 16, No. 2, pp 1208–1218, 2025, https://doi.org/10.11591/ijpeds.v16.i2.pp1208-1218.
17. Z. Medghalchi and O. Taylan, A novel hybrid optimization framework for sizing renewable energy systems integrated with energy storage systems with solar photovoltaics, wind, battery and electrolyzer-fuel cell, *Energy Convers. Manag.*, Vol. 294, p. 117594, 2023, https://doi.org/10.1016/j.enconman.2023.117594.
18. H. Abd El-Sattar, S. Kamel, and M. H. Hassan, A hybrid optimization framework for cost-effective sizing and operation of off-grid hybrid power systems integrated with different storage units, *Int. J. Hydrogen Energy*, Vol. 142, pp 195–220, 2025, https://doi.org/10.1016/j.ijhydene.2025.05.329.
19. I. A. Ibrahim, T. Khatib, and A. Mohamed, Optimal sizing of a standalone photovoltaic system for remote housing electrification using numerical algorithm and improved system models, *Energy*, Vol. 126, pp 392–403, 2017, https://doi.org/10.1016/j.energy.2017.03.053.
20. A. Ali, M. Volatier, and M. Darnon, Optimal Sizing and Assessment of Standalone Photovoltaic Systems for Community Health Centers in Mali, *Solar,* Vol. 3, No. 3, pp 522–543, 2023, https://doi.org/10.3390/solar3030029.
21. N. Shamarova, K. Suslov, P. Ilyushin, and I. Shushpanov, Review of Battery Energy Storage Systems Modeling in Microgrids with Renewables Considering Battery Degradation, *Energies 2022,* Vol. 15, No. 19, 2022, https://doi.org/10.3390/en15196967.
22. S. Loew, A. Anand, and A. Szabo, Economic model predictive control of Li-ion battery cyclic aging via online rainflow-analysis, *Energy Storage*, Vol. 3, No. 3, e228, 2021, https://doi.org/10.1002/est2.228.
23. R. Zieba Falama, Yaouba, F. D. Menga, M. Hamda Soulouknga, F. Kwefeu Mbakop, and C. Ben Salah, A Case Study of an Optimal Detailed Analysis of a Standalone Photovoltaic/Battery System for Electricity Supply in Rural and Remote Areas, *International Transactions on Electrical Energy Systems*, Vol. 2022, No. 1, 7132589, 2022, https://doi.org/10.1155/2022/7132589.
24. R. G. Allwyn, A. Al-Hinai, R. Al-Abri, and A. Malik, Optimization and techno-economic analysis of PV/Battery system for street lighting using genetic algorithm – A case study in Oman, *Clean. Eng. Technol.*, Vol. 8, 100475, 2022, https://doi.org/10.1016/j.clet.2022.100475.
25. M. Andam, J. El Alami, Y. Louartassi, and R. Zine, Days of autonomy for optimal Battery Sizing in Stand-alone Photovoltaic Systems, *Indonesian Journal of Electrical Engineering and Informatics (IJEEI)*, Vol. 11, No. 1, pp 300–317, 2023, https://doi.org/10.52549/ijeei.v11i1.4417.
26. M. Abed, A. Reddy B, T. R. Jyothsna, and N. Mohammed, Optimal sizing and performance assessment of stand-alone PV systems using optimum hybrid sizing strategy, *Results in Engineering*, Vol. 25, 103793, 2025, https://doi.org/10.1016/j.rineng.2024.103793.

27. M. Rynoson, S. Ma Lu, J. Munkhammar, and P. E. Campana, Evaluation of reverse transposition and separation methods for global tilted irradiance: Insights from high-latitude data, *Solar Energy*, Vol. 297, 113597, 2025, https://doi.org/10.1016/J.SOLENER.2025.113597.
28. A. G. Alemu, T. A. Anshebo, and B. B. Dessie, Solar radiation estimation on a tilted surface using sky models in the Afar region of Ethiopia, *Front. Energy Res.*, Vol. 13, 1478555, 2025, https://doi.org/10.3389/FENRG.2025.1478555/BIBTEX.
29. F. E. B. Feitosa and A. L. Costa, Evaluation of Photovoltaic Hydrogen Production Potential Along Highways Connecting the North and Northeast Regions of Brazil, *Journal of Sustainable Development of Energy, Water and Environment Systems*, Vol. 13, No. 2, 2025, https://doi.org/10.13044/J.SDEWES.D13.0574.
30. A. Kaabeche, M. Belhamel, and R. Ibtiouen, Sizing optimization of grid-independent hybrid photovoltaic/wind power generation system, *Energy*, Vol. 36, No. 2, pp 1214–1222, 2011, https://doi.org/10.1016/J.ENERGY.2010.11.024.
31. Layadi T.M., G. Champenois, Etude du vieillissement d'un banc de stockage plomb-acide dans un système hybride multi-sources (In French, Study of the aging of a lead-acid storage bench in a multi-source hybrid system), *Symposium de Génie Électrique 2014 (in French, Electrical Engineering Symposium 2014)*, Jul 2014, Cachan, France, https://hal.archives-ouvertes.fr/hal-01065201, [Accessed: Dec. 07, 2025].
32. D. Yamegueu, H. T. Nelson, and A. S. Boly, Improving the performance of PV/diesel microgrids via integration of a battery energy storage system: the case of Bilgo village in Burkina Faso, *Energy Sustain. Soc.*, Vol. 14, No. 1, pp 1–16, 2024, https://doi.org/10.1186/S13705-024-00480-1/TABLES/3.

Paper submitted: 08.12.2025
Paper revised: 01.04.2026
Paper accepted: 10.04.2026